Impact of the ridge etching-depth on GaSb-based laser diodes

Laura Monge-bartolome, Laurent Cerutti, Eric Tournié

HAL Id: hal-03472735
https://hal.science/hal-03472735

Submitted on 9 Dec 2021

Impact of the ridge etching-depth on GaSb-based laser diodes

Laura Monge-Bartolome, Laurent Cerutti, and Eric Tournié✉ ⓘD

IES University of Montpellier, Montpellier, 34000, France

✉Email: eric.tournie@umontpellier.fr

We have fabricated from the same epitaxial wafer series of GaSb-based Fabry–Pérot laser diodes emitting near 2.3 μm with different ridge etching-depths. The analysis of the device performances allows quantifying the detrimental impact of deep ridge etching. The threshold current density is increased, whereas the external differential quantum efficiency is reduced, due to a reduced internal quantum efficiency and higher optical losses.

Introduction: GaSb-based semiconductor laser diodes (LDs) have progressively emerged as the best suited technology to fabricate devices emitting in the whole 2–3 μm wavelength range, which is of great interest because several molecules exhibit fingerprint absorption lines [1]. Indeed, depending on the objective, threshold current densities below 100 A.cm^{-2}, single mode emission or output powers in the Watt range can all be achieved with the GaSb technology [2, 3]. However, despite the recent progress, there remain parameters to clarify. In particular, the ridge etching-depth has been shown to influence the performance of interband cascade lasers [4, 5]. In this letter we report on the study of the impact of the ridge etching depth on laser diodes.

Epitaxy: The laser structure was grown by solid-source molecular-beam epitaxy on a 2-inch *n*-type (001)-GaSb substrate. The design of the heterostructure is typical for emission near 2.3 μm [2, 3]. Two $Ga_{0.68}In_{0.32}As_{0.09}Sb_{0.91}/Al_{0.25}Ga_{0.75}As_{0.02}Sb_{0.98}$ quantum wells are embedded between 380-nm-thick $Al_{0.25}Ga_{0.75}As_{0.02}Sb_{0.98}$ undoped waveguide layers, whereas the cladding layers are 1.3 μm-thick $Al_{0.85}Ga_{0.15}As_{0.07}Sb_{0.93}$ layers.

Device fabrication: The LDs were fabricated using standard UV photolithography and inductively coupled plasma reactive-ion etching (ICP-RIE) to define the ridges. The ridges were defined either by shallow etching, that is, by etching through the top-cladding layer down to the upper waveguide layer, or by deep etching, that is, by etching through the whole active zone down to the bottom waveguide layer. Electrical insulation and protection were obtained using Si_3N_4 deposited by plasma enhanced chemical vapour deposition (PECVD). Ti-Au and Pd/AuGeNi were used as contact metals for the *p*- and *n*-type electrodes, respectively. Annealing of the metals was performed to ensure low resistance of the *n*-type contact. Note that 10-μm wide ridge LDs with different cavity lengths were cleaved.

Laser characterization: All sets of LDs were tested under continuous wave (cw) operation at room temperature. The output power of the LDs was measured by a calibrated power-meter. We show in Figure 1 the output power-current-voltage (P – I – V) curves taken from a set of deep etched ridge LDs (Figure 1a) and shallow etched ridge LDs (Figure 1b) with four different cavity lengths between 1 mm and 3 mm. The cavity lengths have been measured after cleavage for better accuracy, which explains the slightly different lengths for the two series of LDs. The I – V curves (left axis) show a turn-on voltage around 0.7 V, close to the active zone bandgap, for both series. The serial resistance evolves from 2.5 Ω for the longest diodes to 5 Ω for the shortest ones. The P – I curves (right axis) show that the threshold current evolves from 48 mA for 1.2 mm long diodes to 115 mA for 2.7 mm long ones for deep-ridge LDs, whereas it evolves from 32 mA for 1 mm long diodes to 63 mA for 2.45 mm long ones for shallow-ridge LDs. While the threshold voltage is similar for all deep-etched LDs, it varies slightly for shallow etched LDs due to processing variability.
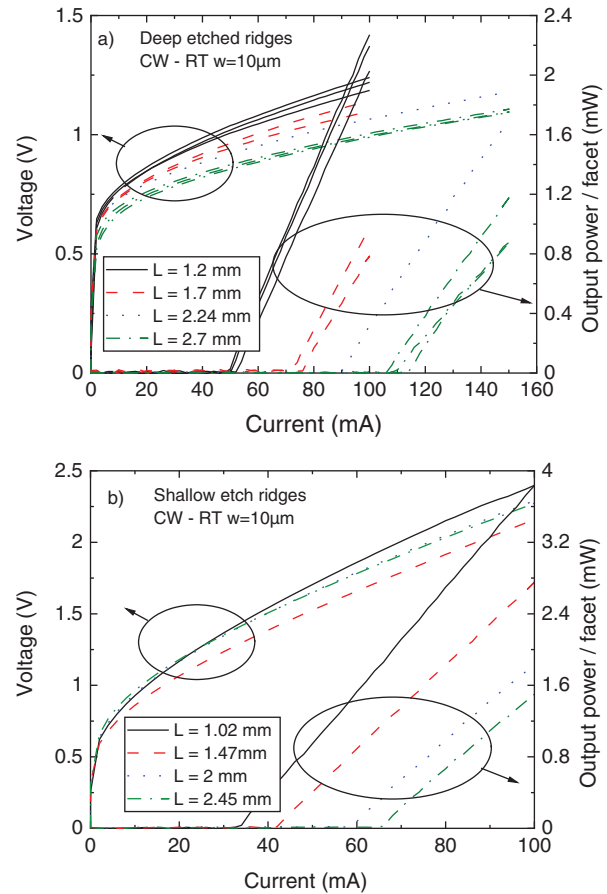

Fig. 1 *P-I-V curves taken under cw operation at room temperature from (a) deep-etched and (b) shallow-etched laser diodes*

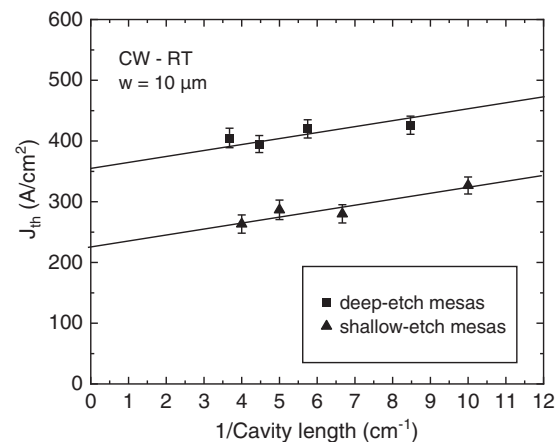**Fig. 2** *Evolution of the threshold current density as a function of the reciprocal cavity length for deep-etched (■) and shallow-etched (▲) laser diodes*

To get a clear view on the influence of the etch depth, we have plotted in Figure 2 the evolution of the threshold current density as a function of the reciprocal cavity length for the two LD series. This evolution can theoretically be fitted by [6]:

$$J_{th} = J_{th}(\infty) - \frac{C}{L}\ln\left(R^{-1}\right) \tag{1}$$

where R is the facet reflectivity, $J_{th}(\infty)$ is the extrapolated current density threshold for an infinite cavity length, L is the cavity length and C is a constant depending on the material system. Two conclusions can be drawn from Figure 2. The two series of datapoints do obey Equation (1) and sit on parallel straight lines, which reveals that both sets of LDs have similar facet reflectivity. On the other hand, the threshold current density
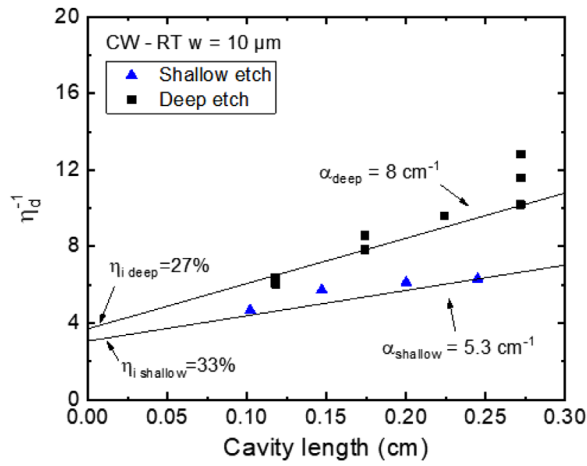
Fig. 3 *Evolution of the reciprocal differential quantum efficiency as a function of cavity length for deep-etched (■) and shallow-etched (▲) laser diodes*

of deep-etch LDs is much higher than that of shallow-etch LDs, the difference being ∼130 A.cm^{-2}, that is, 40–60% of the original threshold.

Next, the external differential quantum efficiencies η_d above threshold have been extracted from the $P - I$ curves and their inverse values are plotted against the cavity length in Figure 3 for both types of cleaved LDs. These data can be analysed using Equation (2) where η_d and η_i are the external differential and internal quantum efficiencies, respectively, R is the facet reflectivity, α_i represents the internal losses and L is the cavity length [7]:

$$\frac{1}{\eta_d} = \frac{1}{\eta_i} + \frac{\alpha_i}{\eta_i \ln (R^{-1})} L. \qquad (2)$$

Both sets of data give slightly different internal quantum efficiencies (27% vs. 33% for deep- and shallow- ridges, respectively). We ascribe the difference to carrier leakage at the deep-ridge side walls. In addition, the slope of the η_d^{-1} *versus* L fit is different for the two data sets. Assuming a power reflectivity of $R = 0.3$ for the facets, one extracts from Figure 3 internal losses of $\alpha_i = 5.3$ cm^{-1} for shallow-ridge LDs, a typical value for LDs made in this materials system [2, 3]. In contrast, the slope gives a value of $\alpha_i = 8$ cm^{-1} for the deep-ridge LDs. These differences arise from non-radiative recombination and optical losses through scattering at the side walls of deep-ridge LDs.

Conclusion: We have fabricated and studied different series of GaSb-based quantum-well LDs with deep and shallow etched ridges. Our results show that deep ridge etching increases the internal losses and lowers the internal quantum efficiencies, which results in higher threshold current densities and lower external differential quantum efficiencies.

Data availability statement: The data that support the findings of this study are available from the corresponding author upon reasonable request.

References

1 Gordon, I.E. et al.: The HITRAN2016 molecular spectroscopic database. *J. Quant. Spectrosc. Radiat. Transf.* **203**, 3–69 (2017)

2 Belenky, G., Shterengas, L., Kisin, M.V., Hosoda, T.: Gallium antimonide (GaSb)-based type-I quantum well diode lasers: recent development and prospects. In: Baranov, A.N., Tournié, E. (eds.) *Semiconductor Lasers*. Elsevier, Amsterdam, pp. 441–486 (2013)

3 Cerutti, L., Vicet, A., Tournié, E.: Interband mid-infrared lasers. In: Tournié, E. Cerutti, L. (eds.) *Mid-infrared Optoelectronics*. Elsevier, Amsterdam, pp. 91–130 (2020)

4 Forouhar, S. et al.: Reliable mid-infrared laterally-coupled distributed-feedback interband cascade lasers. *Appl. Phys. Lett.* **105**(5), 051110 (2014).

5 Feng, T., Hosoda, T., Shterengas, L., Stein, A., Kipshidze, G., Belenky, G.: Two-Step Narrow Ridge Cascade Diode Lasers Emitting Near 2 μm. *IEEE Photonics Technol. Lett.* **29**(6), 485–488, (2017)

6 Yang, J., Mi, Z., Bhattacharya, P.: Groove-coupled InGaAs/GaAs quantum dot laser/waveguide on silicon. *J. Light. Technol.* **25**(7), 1826–1831 (2007)

7 Coldren, L.A., Corzine, S.W., Mašanović, M.L.: *Diode Lasers and Photonic Integrated Circuits*. John Wiley & Sons, Hoboken, NJ (2012)